3D-printable cell crowding device enables imaging of live cells in compression

Supplementary Materials

Strain mapping analysis

To determine substrate strain, two different software packages were used. In each case, two images obtained under different numbers of revolutions of the lead screw and thus different strain states were compared; the results obtained using the two packages are fully consistent. Images were converted to 8-bit grayscale and analyzed via cross-correlation analysis to determine the displacement field within the substrate. Here we report the displacement direction and semi-quantitative strain magnitude obtained using MATLAB PIVlab 2.02 (MathWorks) (Fig 2A, left). Further quantification of the strain field was performed using the PIV plug-in in ImageJ. Using the cross-correlation mode, we calculated the displacement field using iterative window sizing (typically 128, 64, 32 pixels or 512, 256, 128 pixels; Fig. 2A, right). The substrate displacement was then measured by averaging the lateral displacement of the center portion of the silicone sheet; typically 5-10 *y*-displacement values were averaged for each *x*-position. We plotted this line-averaged *x*-displacement versus *x*-position and determined the local strain from a linear fit to the resultant data (Fig. 2B). This was repeated for several different numbers of revolutions. We found a linear relationship between the lateral strain and the number of revolutions of the lead screw, with 0.016 lateral strain units achieved per turn (Fig. 2C). Although it is not possible to use open-source DIC analysis to determine large sample strains, as the cross-correlation method becomes increasingly inaccurate when the displacements between the image pairs is large. We have confirmed that this linear relationship persists for at least 21 turns of the lead screw, corresponding to ~34% strain.

Substrate properties and functionalization

To promote cell attachment, a narrow strip of .02-inch-thick gloss silicone rubber (Specialty Manufacturing Inc., Saginaw, MI) was cut into a section 8-9 mm wide and approximately 15 cm long. Per the manufacturer, the silicone sheet is formed from SILASTIC BioMedical Grade Liquid Silicone Rubber type Q7-4840, with a 5-minute press cure and no post cure processing. Per Dow Corning, the typical modulus for this material at 200% is 2.6 MPa. We measured a slightly lower value experimentally of ~1.9 MPa (for strains <5%). However, the device operates in a displacement-controlled mode, so the substrate modulus value is not particularly important to is operation, as long as the device is capable of applying enough force to achieve the desired displacement. The substrate was then sonicated in 70% ethanol for 10 minutes, rinsed with 100% ethanol, blown dry with nitrogen gas, and plasma treated at 18W for 10 minutes using a plasma cleaner with ambient room air at low pressure ~ 150 milliTorr (PDC-32G, Harrick Plasma, Ithaca, NY). Upon surface treatment, 100 µg/mL of human fibronectin (Sigma Aldrich, F2006) was added to the central region of the silicone strip and allowed to incubate overnight at room temperature.

Device Sterilization

The device was thoroughly wiped with 70% ethanol and placed within a biosafety cabinet for silicone strip clamping, along with cell seeding. We recommend UV exposure as an appropriate sterilization technique, but advise against autoclaving the device as the glass transition temperature of ABS is ~105 ˚C [1], significantly lower than the standard autoclaving temperatures of ~121 ˚C.

Cell Culture

A concentrated cell suspension was prepared from a 100% confluent monolayer of eGFP E-cadherin MDCKII cells cultured in a T25 vented flask with 5% CO_2 at 37°C. The culture medium consisted of Dulbecco's Modified Eagle Medium (DMEM) (ThermoFisher, 12430054), 10% Fetal Bovine Serum (FBS) (Life Technologies, 10437028), and 1% Penicillin Streptomycin (PS) (Life Technologies, 15140122).

Imaging

Imaging was performed using an inverted Leica TCS-SP8 spectral confocal microscope with a 10X air objective (numerical aperture, NA = 0.3), at an 8,000 Hz scan speed, with a pinhole diameter of 1 AU. Imaging medium used was phenol red free DMEM (ThermoFisher # 21063029), supplemented with 15 mM HEPES, 10% FBS, and 1% PS. A field of view near the center of the silicone sheet was manually identified and imaged using bidirectional line-sequential scans (LineAverage=16). The first scan used 405-nm excitation with a 410-483-nm detection window to image the Hoechst-stained nuclei (10 µM Hoechst stain; ThermoFisher # H3570). The second scan used a white light laser (WLL) providing 488 nm excitation with a 493-549-nm detection window to image the GFP-cadherin. For each location, a field of view with typical in-plane area of 155×155 μm^2 (corresponding to 800×800 $pixels^2$) and 59 .0 µm stack height (along the optical axis *z*) was imaged; each scan took approximately 2 minutes to collect. This resulted in a stack of 60 2D images with an approximate difference 1 µm between z-planes.

Quantification of cell crowding

To assess the changes in cell shape in response to compression, the GFP channel was isolated using Fiji/ImageJ. The heights and widths of 40 randomly selected cells were then manually measured using the line segment tool in Fiji/ImageJ, averaged, and the aspect ratio calculated. Cell density along the compressive axis was first determined by isolating the Hoechst channel, creating a maximum intensity projection of the *z*-stack, smoothing the image with the "smooth" tool in Fiji.ImageJ, then converting to an 8-bit binary image. Five random line segments were drawn horizontally across the image and the grayscale intensity profile was plotted using Fiji/ImageJ. Peaks, indicating the presence of a nucleus, were summed for each plot and averaged for the five line segments (Fig. S1).

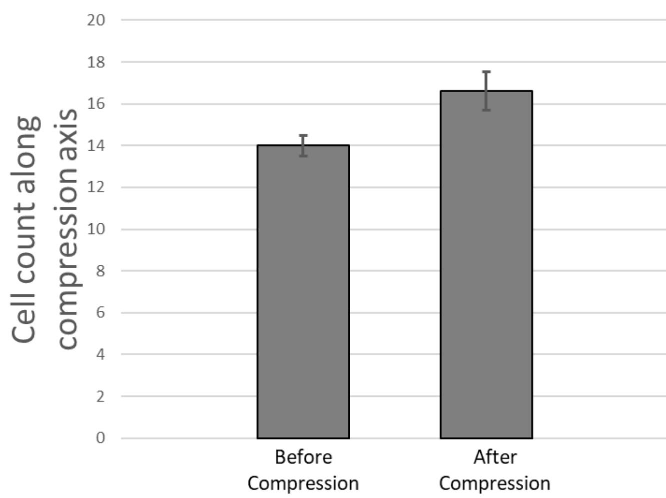

Figure S1. Cell density along the axis of compression increased approximately 20%, from 14.0 ± 0.5 to 16.6 ± 0.9. Error bars indicate standard error of the mean. Cells were counted using the maximum intensity projections of the Hoechst channel before and after crowding.

Materials List and Assembly Instructions

Table S1: 3-D Printed Parts			
Printer/material	Part Description	Annotation Number	Quantity
Stratasys f270/ABS	Base	1	1
Stratasys f270/ABS	Clamp	2	2
Stratasys f270/ABS	Clamp Holder-RH	3	1
Stratasys f270/ABS	Clamp Holder-LH	4	1
Stratasys f270/ABS	Indenter	5	1
Stratasys f270/ABS	Dish Holder	6	1
Stratasys f270/ABS	Lid	7	1
Table S2: McMaster-Carr Parts			
Catalog Number	Part Description	Annotation Number	Quantity
97372A106	LH to RH coupling nut	8	1
90036A029	LH rod machined with 8-32 threads	9	1
98837A029	RH rod machined with 8-32 threads	10	1
6061K101	1/4” diameter, 8” long dowel	11	1
90519A029	Left hand nut	12	1
90490A029	Right hand nut	13	1
94510A040	M4 Brass threaded insert	14	4
92855A413	M4 12mm long screw	15	4
57155K371	¼” ball bearing	16	2
5993K11	8-32 threaded knob	17	2
98380A431	Roller dowel pin	18	2
92320A475	Dowel pin unthreaded spacer	19	2
6489K61	¼” linear ball bearing	20	2
98055A381	Shim used for magnetic attachment	21	1
5862K961	Magnet	22	4
98380A429	Indenter dowel	23	2
92321A014	Indenter roller	24	2

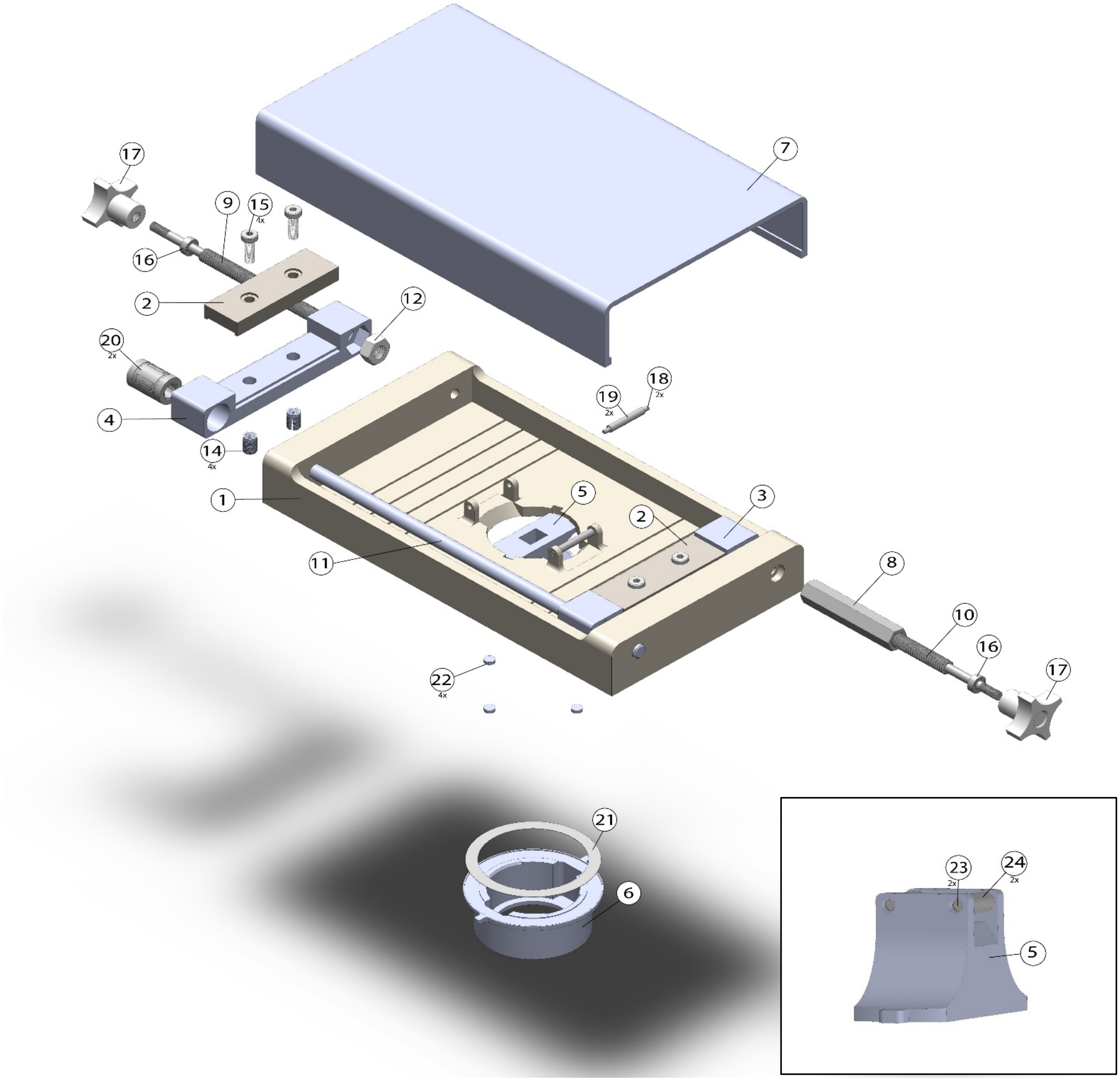

Figure S2: Exploded view of the assembled device, with annotation numbers as described in Tables S1 and S2. Since some regions of this device experience high localized stress during tension, the 3-D printed components included structural support features such as side ribs (1) for the base plate and gussets for the indenter (5, in inset).

Instructions for assembly

1. Print the accompanying STL files with a 3-D printer capable of printing structural resins that can withstand high thermal stress (e.g. we used the Stratasys f270 which was capable of fused deposition modeling to print acrylonitrile butadiene styrene).
2. Purchase or obtain the necessary parts listed in the table above.
    a. The only parts that need to be modified are the threaded rods (#90036A029 and #98837A029). See instruction below

Left-hand threaded rod

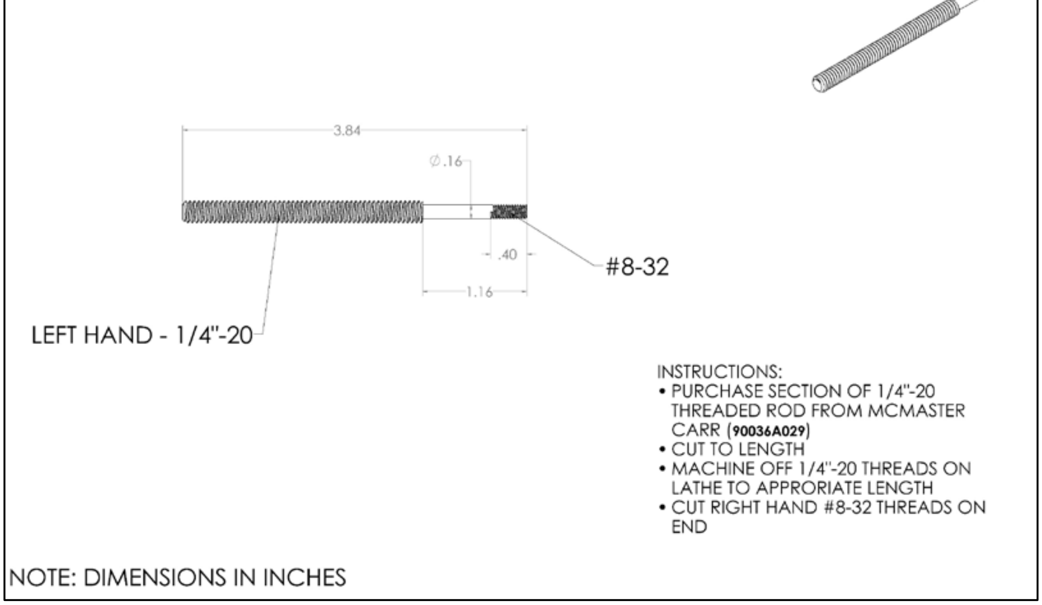

Right-hand threaded rod

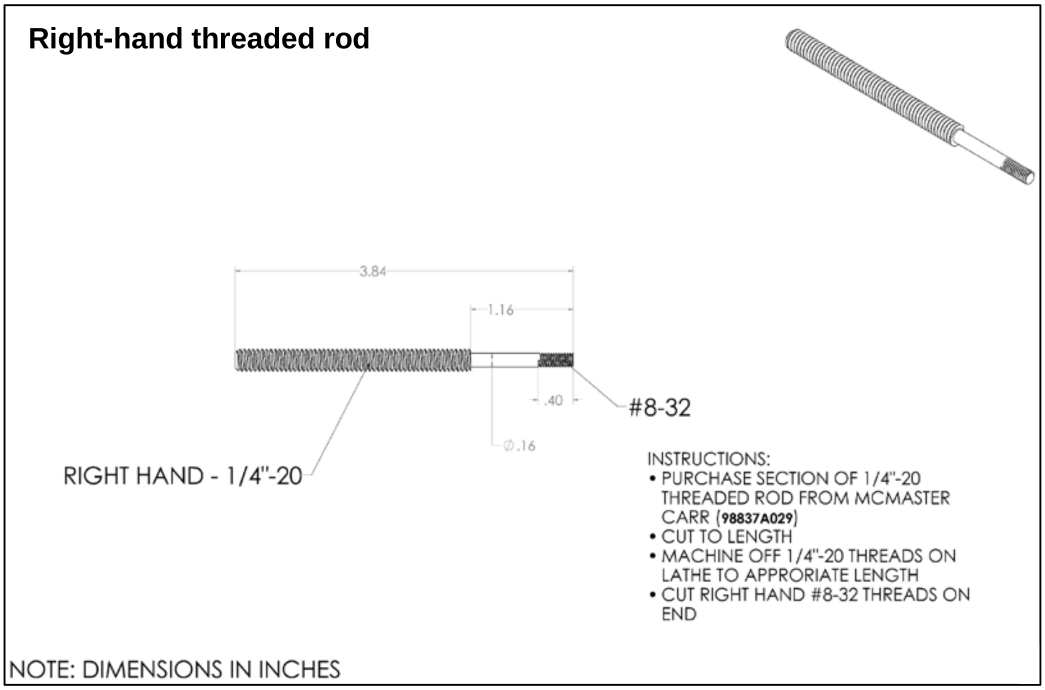

b. **Assemble clamp holders**
   i. For the LH clamp holder, glue the LH nut (90519A029) into the hexagonal opening and the ¼” linear ball bearing (6489K61) into the larger opening on the other side.
   ii. Repeat the above step for the RH clamp holder, except replace the LH nut with the RH nut (90490A029).
   iii. Insert, with glue, a brass threaded insert (94510A040) into both holes in the middle of the clamp holder.
      1. *Note: you may need a hammer to get it fully seated*
   iv. Allow glue to dry.

c. **Assembling the lead screw through the clamp holders**

   i. On both sides of the base plate, insert the ¼” ball bearing (57155K371) inside the 5/16” opening. Depending on the fit, you may need a rubber mallet (if too tight) or a little glue (if too loose).

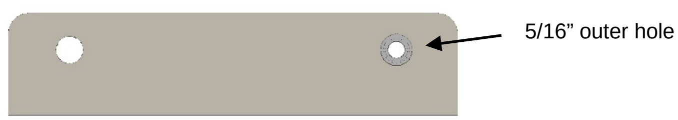

   ii. Place both clamp holders inside the base plate so that the LH and RH nuts are aligned and face the center while lining up with the 5/16” outer hole.

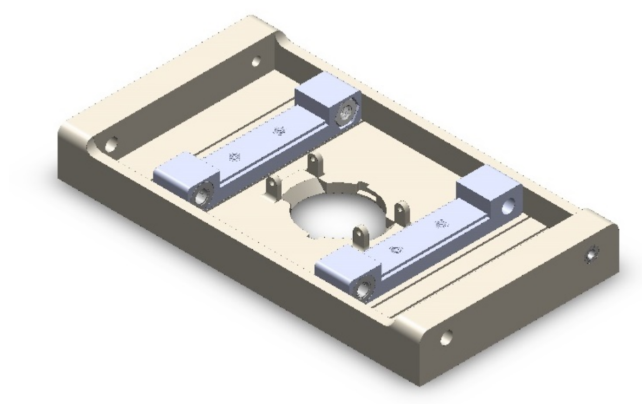

   iii. To assemble the lead screw, thread the RH and LH threaded rods from the inside into their respective nuts

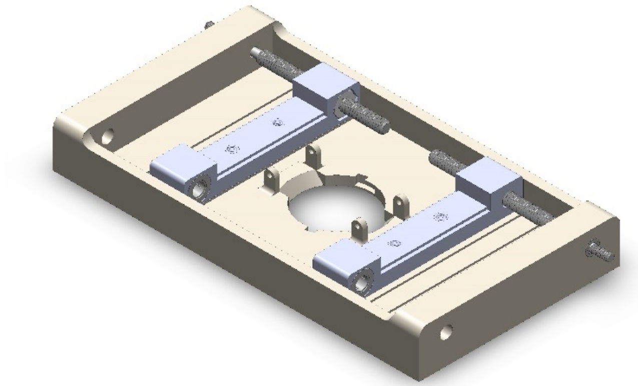

iv. Screw both rods into the LH to RH coupling nut (97372A106) while making sure the clamp holders are centered. After this step, you can test your device by turning the lead screw and making sure that the clamp holders move between the middle and edges of the base plate equidistantly. Only then should you proceed to the next step.
   Note: This step requires extra attention: Make sure that the threaded rods are pulled as far back as possible so that you have clearance to fasten the nut. Also make sure you secure them tightly so that the assembly turns together and does not unscrew. Glue may help here.

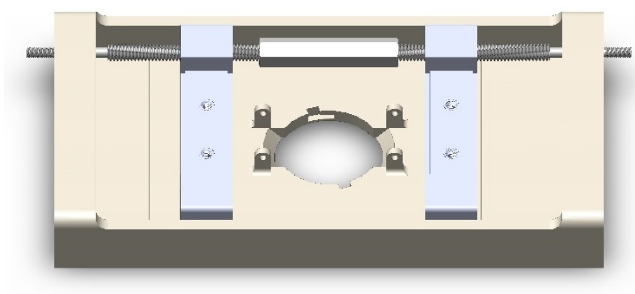

v. Finish assembling the lead screw by attaching an 8-32 thread knob (5993K11) to the outer ends.

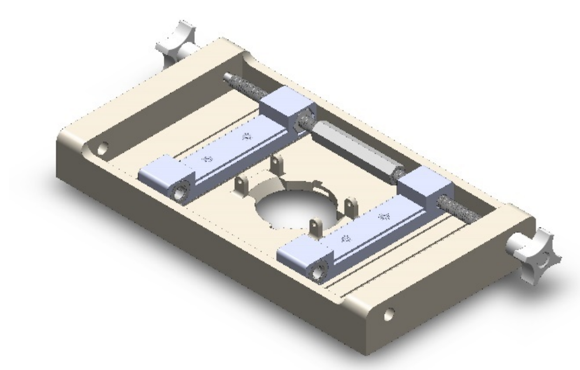

d. Insert the ¼” diameter, 8” long dowel (6061K101) through the opposite ends of the clamp holders. Use glue on the outside to fix the rod in place.

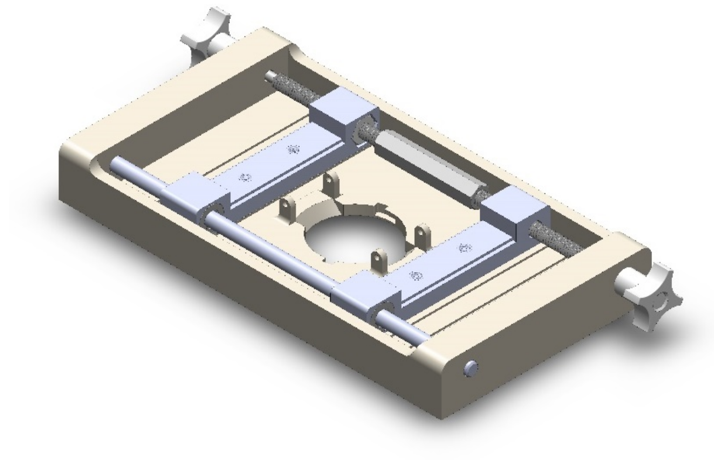

e. Insert the stainless-steel dowel pin (98380A431) through the unthreaded spacer (92320A475) and fix, using glue, the two ends of the dowel pin between the respective holes on top of the base plate. Repeat for the other side.

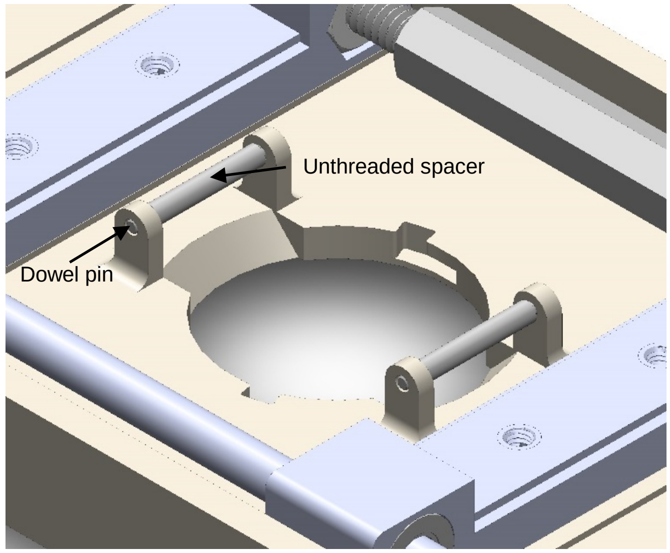

f. Flip device over and glue in the 4 magnets (5862K961)

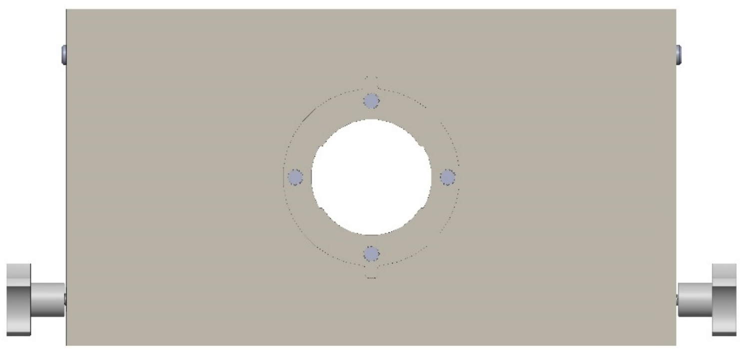

g. Glue the magnetic circular shim within the corresponding indented region of the 3-D printed dish holder. Once the glue is dried, the dish holder should now magnetically attach to the base plate.

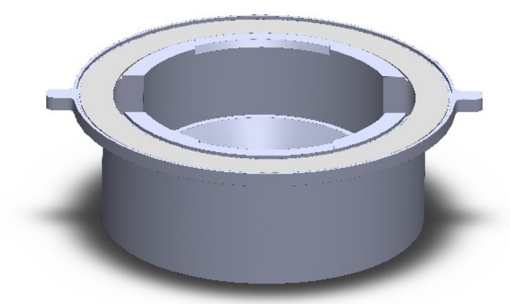

h. In a similar fashion as step e, insert the 0.5” stainless-steel dowel pin (98380A429) through the unthreaded spacer (92321A014) and fix, using glue, the two ends of the dowel pin between the respective holes on the 3-D printed indenter. Repeat for the other side.

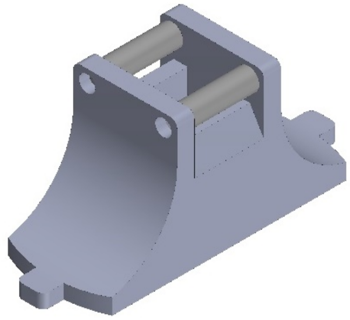

i. To insert the indenter into the base plate, flip over and insert the tabs into the corresponding inserts of the base plate. Twist to lock in place.

Note: In the event of a loose fit, you can cap the ends of the indenter tabs with parafilm to provide a tight fit.

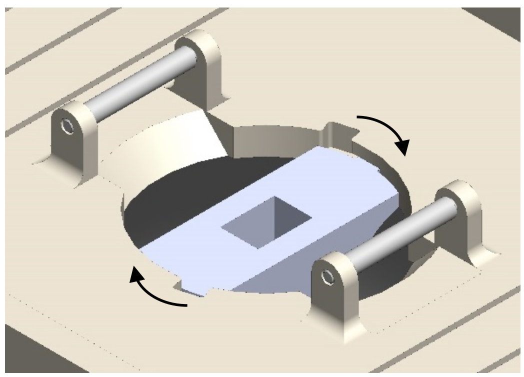

j. When threading a deformable silicone substrate within the device for experiments, screw the clamps into the clamp holders using two M4 12 mm screws (92855A413) per clamp.

Note: For better traction or if slippage occurs, adhere a thin rough material (e.g. sandpaper) to the top of the clamp holder and on the underside of the clamp.

k. A schematic of the final assembled device is shown below. Images are provided in Fig. 1.

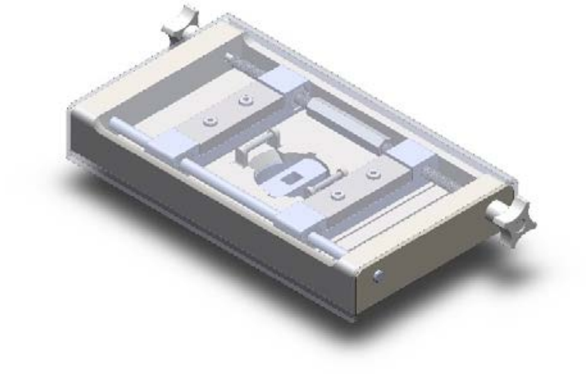

References

1. Typical Properties Generic ABS.[online], 2016,[cit. 2016-04-30]. *Dostupné na: http://plastics. ulprospector. com/generics/1/c/t/acrylonitrile-butadiene-styrene-abs-properties-processing*.